EEET ECOLOGICAL ENGINEERING & ENVIRONMENTAL TECHNOLOGY

Ecological Engineering & Environmental Technology, 2026, 27(7), 405–418
https://doi.org/10.12912/27197050/224508
ISSN 2719–7050, License CC-BY 4.0

Received: 2026.05.31
Accepted: 2026.06.15
Published: 2026.07.01

Waste valorization of spent coffee grounds as eco-friendly biofiller in polypropylene biocomposites: Effect of alkali treatment on mechanical, rheological, and physical properties with statistical analysis regression modeling

Kaouthar Boumane[1*], Mostapha Karaoui[1], Naima Moustaghfir[1], Mohammed Alami[1], Mohammed Assouag[1]

[1] Team of Innovative Materials and Mechanical Manufacturing Processes, ENSAM, University Moulay Ismail, B.P. 15290, Al Mansour, Meknes, Morocco
* Corresponding author's e-mail: ka.boumane@edu.umi.ac.ma

ABSTRACT

Spent coffee grounds (SCG) represent a high volume agro-industrial waste stream generated globally, and their valorization as biofillers in thermoplastic composites offers a promising pathway for waste reduction and sustainable material development. This study examines the influence of alkali treatment and filler loading (5, 10, 15, and 20 wt%) on the physical, rheological, and mechanical behavior of polypropylene (PP) composites reinforced with SCG. Composites were produced by injection molding and characterized in terms of density, melt flow index (MFI), Shore D hardness, and tensile properties. One-way ANOVA (Analysis of variance) confirmed statistically significant differences among all formulations for every measured property ($p < 0.05$), and Tukey's honestly significant difference (HSD) post hoc tests ($\alpha = 0.05$) were applied to identify homogeneous subsets. Alkali treatment improved SCG surface roughness and interfacial adhesion with the PP matrix, as confirmed by optical microscopy. Mechanically, treated composites retained tensile strength close to neat PP at low filler loadings (38.6–40.5 MPa at 5–10 wt%), while hardness increased progressively, reaching 66.96 Shore D at 20 wt%. The MFI dropped by approximately 31% for untreated composites and approximately 75% for treated ones at 20 wt%, relative to neat PP (17.03 g/10 min). Composite density increased by up to 6.6% with SCG addition. Four regression models were fitted to each measured property; quadratic models yielded the highest R^2 values for most parameters, while elongation at break followed a linear trend. Treated composites consistently showed higher R^2 values than untreated ones, confirming that surface treatment improves the predictability of composite behavior. These results demonstrate that SCG can be effectively valorized as an eco-friendly biofiller in PP-based materials, contributing to both waste reduction and the development of more sustainable composites.

Keywords: biocomposites, polypropylene, spent coffee grounds, waste valorization, alkali treatment, injection molding, regression modeling.

INTRODUCTION

Growing environmental awareness and the need to reduce dependence on petroleum-derived materials have driven considerable interest in polymer-based biocomposites, which combine synthetic matrices with natural or waste-derived fillers to achieve a more sustainable balance between performance and ecological impact (Raj et al., 2021; Väisänen et al., 2016). Some formulations also show potential in packaging applications where reduced environmental impact is a priority (Kamarudin et al., 2022). For structural applications, natural fiber reinforced hybrid polymer composites offer superior mechanical performance, making them suitable for demanding uses while reducing dependence on petroleum-based polymers (Nurazzi et al., 2021). Furthermore, natural fiber reinforced polymer composites are increasingly recognized for their

sustainability, as they combine renewable resources with flexible manufacturing processes to produce lightweight and strong materials (Kamarudin, Mohd Basri, et al., 2022).

Among thermoplastic matrices, polypropylene (PP) stands out for its favorable combination of mechanical performance, processability, and cost, which has made it a material of choice across the automotive, packaging, and construction sectors (Liao et al., 2019). Natural fibers are attracting growing interest as reinforcements in PP-based composites due to their renewable, biodegradable, and economical nature (McKay et al., 2024; Vigneshwaran et al., 2020). Their incorporation not only improves stiffness and specific strength, but also reduces the environmental footprint of PP-based materials (Khoathane et al., 2008). Processing conditions play a decisive role in the interfacial adhesion and overall mechanical performance of these composites (Qaiss et al., 2015). Recent advances, notably the alkaline treatment of natural fibers, have proven effective in improving interfacial adhesion and mechanical performance in PP-based biocomposites (Osman et al., 2025).

Among bio-based fillers, SCG have attracted particular interest due to the scale of their global production and the practical challenges associated with their disposal. Their lignocellulosic composition rich in cellulose, hemicellulose, and lignin makes them structurally relevant as reinforcing agents, and their abundance positions them as an accessible, low-cost biofiller for thermoplastic applications (Campos-Vega et al., 2015; Hernández-Varela and Medina, 2023). Studies on PP-based composites have revealed an increase in stiffness, accompanied by a decrease in tensile strength and elongation at break, particularly when the SCG remained untreated. Alkaline treatment has improved these properties by enhancing interfacial adhesion (Thanh et al., 2023).

Surface modification through alkaline treatment has proven to be one of the most practical and cost-effective approaches for improving fiber-matrix compatibility in PP-based biocomposites. By partially removing lignin, waxes, and surface impurities, NaOH treatment increases surface roughness and exposes more reactive hydroxyl groups, which promotes mechanical interlocking and chemical affinity at the interface (Osman et al., 2025; Xiao et al., 2022).

Despite this body of work, several critical gaps remain unaddressed in the literature. First, most PP/SCG studies report experimental property values at fixed filler loadings without applying regression modeling to quantify how filler content continuously drives property evolution. Second, the statistical significance of property differences between untreated and alkali-treated formulations is rarely assessed through rigorous inferential frameworks, limiting the reproducibility and comparability of reported results. Third, a systematic head-to-head comparison of untreated versus alkali-treated SCG across multiple regression frameworks has not been reported, leaving the question of whether surface treatment improves the regularity and predictability of composite behavior unresolved.

The present study seeks to fill these gaps by investigating the effects of alkali surface treatment and filler loading (5, 10, 15, and 20 wt%) on the mechanical, rheological, and physical performance of injection-molded PP/SCG biocomposites. The central scientific hypothesis is that alkali surface treatment fundamentally alters the predictability and regularity of property evolution by promoting more uniform filler dispersion and limiting particle agglomeration within the polymer matrix. Consequently, the primary objective of this work is to identify and validate the underlying mathematical patterns linear, quadratic, logarithmic, or exponential governing these property transitions as a function of filler content. By determining the most appropriate predictive frameworks for each property, this study aims to provide a quantitative modeling approach that bridges empirical observation and reliable engineering design of sustainable PP-based biocomposites.

MATERIALS AND METHODS

Materials

The polymer matrix is a commercial PP homopolymer (Al Waha Petrochemical Company, Jubail, Saudi Arabia) supplied as white granules with a density of 0.90 g/cm³.

Preparation of spent coffee grounds (SCG)

Untreated spent coffee grounds

SCG were collected from a cafeteria in Meknes, Morocco. The material was washed with hot water to remove impurities and oils, rinsed

with cold water, oven-dried, and sieved to obtain particles with an average size of 63 µm.

Alkaline treatment of spent coffee grounds

Dried SCG were immersed in an 8 wt% NaOH solution at room temperature for 24 hours. After treatment, the SCG were filtered, washed repeatedly with distilled water until neutral pH, dried at 60 °C for 12 hours, and sieved through a 63 µm mesh (Thanh et al., 2023).

Manufacturing of PP composites

PP-based composites, reinforced with treated and untreated SCG, were manufactured using an injection molding machine BTW 1400-S (Beston Group V1400-410, Ningbo, Zhejiang, China). The processing parameters included a temperature range of 180–210 °C, an injection pressure of 30 bar, and an injection velocity of 20 mm/s (Karaoui et al., 2025). The composition of the PP/SCG composites is presented in Table 1.

Experimental procedure

Optical microscopy

Optical microscopy was performed using a JSM-IT500HR In Touch Scope™ microscope (JEOL Ltd., Tokyo, Japan) to analyze the dispersion behavior of SCG within the PP matrix (Karaoui et al., 2025).

Mechanical properties

Tensile tests were performed using a universal testing machine model EM0-20KN equipped with a 500 N load cell (ERM Fab and Test, Carpentras, France), operating at a crosshead speed of 30 mm/min and a temperature of 23 °C, in accordance with ISO 527-2type 5A (International Organization for Standardization, 2012). The reduced section of the specimens had dimensions of 25 × 4 × 2 mm (length × width × thickness), and representative specimens are presented in Figure 1. Five replicate specimens were tested per condition, in line with standard practice for mechanical testing of polymer composites. The stress-strain curves generated served to determine Young's modulus, tensile strength, and tensile strain.

Hardness measurements were carried out using a Shore D Durometer (Innovatest Europe BV, Borgharenweg Maastricht, The Netherlands), in accordance with the NF EN ISO 868 standard (International Organization for Standardization (ISO), 2003). For each sample, five measurements were taken, and the software of the instrument automatically computed the mean hardness value.

Melt flow index (MFI)

The flow behavior was evaluated using a Tinius Olsen MP1200 melt flow tester (Tinius Olsen Ltd., Horsham, PA, USA), according to ASTM D1238, ISO 1133-1 (International Organization for Standardization (ISO), 2022), and ISO 1133-2 standards (International Organization for Standardization (ISO), 2011). Granular samples were loaded into the barrel at 230°C under a 2.16 kg load, and the mass of polymer extruded over a given time was measured. The MFI was calculated using Equation 1:

$$MFI\ (g/10\ min) = m \times t_r / t_e \quad (1)$$

where: m represents the mass of extrudate, t_r corresponds to the reference time, and t_e is the extrusion time.

Each measurement was repeated three times, and the average value was reported.

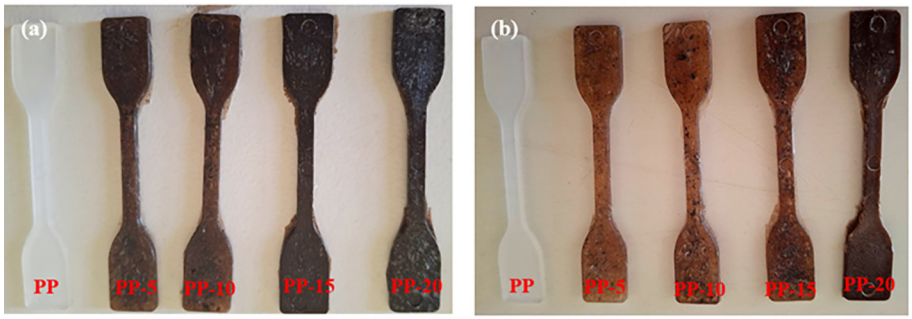

Figure 1. Images of PP specimens incorporated with varying amounts of untreated spent coffee ground: (a) untreated, (b) treated

Table 1. Composition of fabricated PP-based composites reinforced with SCG

Sample	SCG content (wt%)	PP content (wt%)
PP	0	100
PP/SCG-5%	5	95
PP/SCG-10%	10	90
PP/SCG-15%	15	85
PP/SCG-20%	20	80

Density

Density assessments were carried out following ISO 1183 (International Organization for Standardization (ISO), 2006), utilizing a ZLS 220A SCS densitometer (ZwickRoell, Ulm, Germany). Each sample was first measured in air mode, then its submerged density was determined by immersion in distilled water. The average of three separate specimens was reported.

Statistical analysis and regression modeling

Statistical analyses and regression modeling were performed using RStudio and OriginPro. For each measured property, means and standard deviations were computed from five replicates per formulation. One-way ANOVA was applied to assess the significance of differences among formulations, and when significant effects were detected, Tukey's HSD post hoc test was conducted at a significance level of ($\alpha = 0.05$) to identify statistically homogeneous subsets. Group membership was denoted by lowercase letters, with different letters indicating statistically significant differences between means.

To quantify the relationship between SCG content and composite properties, four regression models were fitted to the experimental data: linear, quadratic, exponential, and logarithmic. The coefficient of determination (R^2) was used as the primary goodness-of-fit criterion to identify the model best describing property evolution as a function of filler loading.

RESULTS AND DISCUSSION

Visual aspect and optical microscopy

After incorporation of the filler, the appearance of the biocomposites was altered progressively, with filled specimens exhibiting darker coloration compared to pure PP (Figure 1). The darkening with increasing SCG content can be attributed to the lignocellulosic particles within the polymer matrix, which create irregular regions with varying refractive indices and dark absorption zones. Alkaline treatment partially removes lignin, oils, and phenolic pigments, resulting in lighter and more homogeneous composites. Similar observations were reported by (Ortiz-Barajas et al., 2020) for polylactide composites incorporating torrefied coffee husk flour, and (Stelea et al., 2022) for hemp-fiber-reinforced thermoplastic composites.

Optical microscopy images (Figures 2 and 3) confirm that untreated SCG composites exhibit more heterogeneous filler dispersion at higher loadings, with visible agglomerates that act as stress concentration points. Treated composites show smaller, more uniformly distributed particles, attributable to the removal of surface impurities by NaOH treatment, which improves interfacial adhesion with the PP matrix (Osman et al., 2025; Xiao et al., 2022).

General properties of PP/SCG biocomposites

Table 2 summarizes the mean values and standard deviations of all measured properties for each composite formulation. One-way ANOVA confirmed statistically significant differences among groups for all parameters ($p < 0.05$), and post hoc Tukey HSD tests were applied to identify homogeneous subsets ($\alpha = 0.05$).

Tensile properties

Figure 4 illustrates the effect of SCG incorporation and alkali surface treatment on the Young's modulus of the biocomposites. One-way ANOVA reveals that both filler loading and chemical modification exert a highly significant effect on material stiffness ($p < 0.001$; $F = 42.11$). Post hoc Tukey's HSD test confirms that alkali-treated composites at 5–15 wt% share the same superior statistical subset as neat PP (group 'a'), indicating that stiffness was effectively maintained within this concentration range. This behavior is consistent with improved filler-matrix interaction and a satisfactory dispersion state, which may facilitate stress transfer throughout the composite structure (Vilaseca et al., 2010). Untreated formulations follow a distinct statistical path: a significant stiffness drop is observed at 5 wt% Untreated

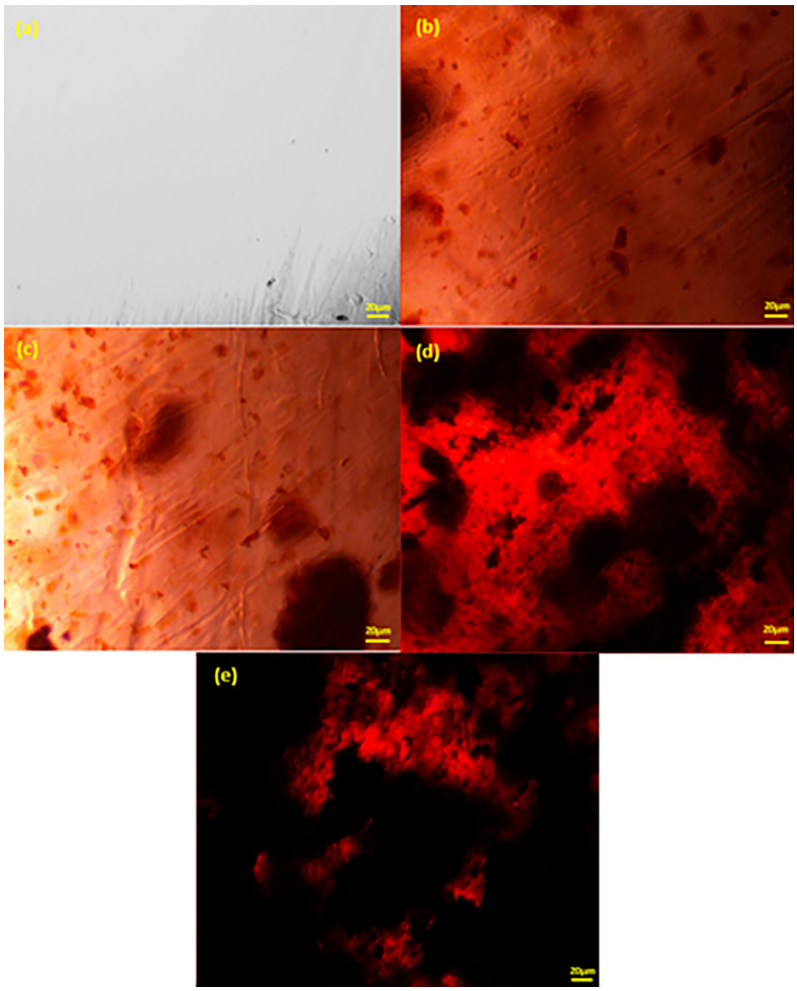

Figure 2. Microscope optical images of untreated SCG and PP/SCG composites: (a) PP, (b) PP/SCG-5, (c) PP/SCG-10, (d) PP/SCG-15, and (e) PP/SCG-20

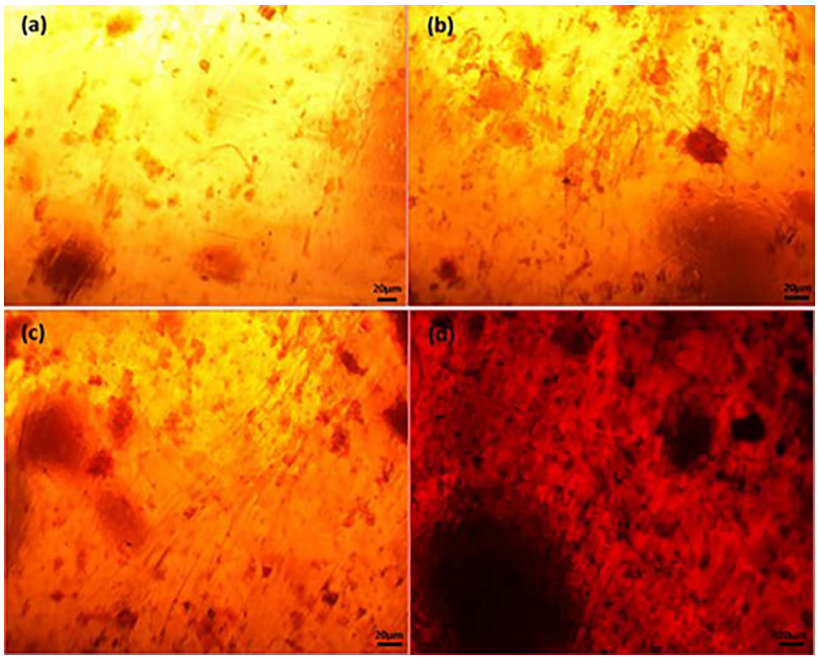

Figure 3. Microscope optical images of treated SCG and PP/SCG composites: (a) PP/SCG-5, (b) PP/SCG-10, (c) PP/SCG-15, and (d) PP/SCG-20

Table 2. Mechanical, physical, and rheological properties of PP/SCG biocomposites

Formulation		Mechanical properties				Physical and rheological properties	
		Young's modulus (GPa)	Tensile strength (MPa)	Strain (%)	Hardness (Shore D)	MFI (g/10min)	Density (g/cm³)
PP		0.9514 ±0.026	40.15 ±1.97388	0.3366 ±0.055	61.20 ±0.26	17.03 ±2.56	0.9037 ±0.0015
PP/SCG-5%	Untreated	0.8260 ±0.0456	39.9 ±0.624	0.185 ±0.078	61.70 ±0.20	13.87 ±1.87	0.922 ±0.0046
	Treated	1.0062 ±0.0484	38.6 ±0.71	0.1395 ±0.025	64.57 ±2.968	10.72 ±1.52	0.9087 ±0.0051
PP/SCG-10%	Untreated	0.8796 ±0.0606	37.62 ±2.29	0.161 ±0.049	62.83 ±0.305	11.92 ±2.27	0.9297 ±0.0042
	Treated	1.0248 ±0.0561	40.47 ±2.804	0.181 ±0.021	65.43 ±0.808	9.20 ±1.52	0.9107 ±0.0097
PP/SCG-15%	Untreated	0.8862 ±0.057	36.76 ±2.819	0.1618 ±0.021	63.27 ±0.251	11.84 ±0.84	0.9587 ±0.0155
	Treated	1.0196 ±0.0532	35.175 ±0.796	0.1142 ±0.011	66.43 ±1.8903	4.88 ±1.685	0.9370 ±0.0053
PP/SCG-20%	Untreated	0.6894 ±0.0292	31.89 ±2.635	0.0420 ±0.019	63.3 ±0.80	11.76 ±0.87	0.9610 ±0.0132
	Treated	0.662 ±0.0309	30.84 ±1.1898	0.1776 ±0.005	66.97 ±2.41	4.24 ±0.692	0.9587 ±0.0025
ANOVA(p-value)		5.55E-16	1.74E-10	3.73E-8	0.001	4.0533E-7	5.7103E-8

Note: Values are presented as mean ± SD (standard deviation) based on five replicates per formulation. p-values are derived from one-way ANOVA.

(group 'b'), followed by a partial recovery at 10–15 wt% treated (group 'ab'), where the higher volume fraction of rigid lignocellulosic particles partly compensates for poor interfacial adhesion. At 20 wt%, both treated and untreated composites collapse into the same lower statistical subset (group 'c'), attributed to particle agglomeration and micro-void formation disrupting matrix homogeneity consistent with findings reported by (Serra-Parareda et al., 2021) for PP composites reinforced with henequen fibers.

The evolution of the composite tensile strength is presented in Figure 5. ANOVA confirmed a highly significant variation in the maximum load-bearing capacities ($p < 0.001$; $F = 17.65$). Tukey's post-hoc analysis demonstrates that while the neat polymer exhibits the highest tensile strength (~40 MPa), it remains statistically identical to the 5 wt.% untreated, 5 and 10 wt.% treated formulations, which share the same dominant statistical family (group 'a'). This statistical equivalence indicates that the incorporation of SCG at low filler contents did not significantly compromise the tensile strength of the PP matrix. This behavior may be associated with a relatively satisfactory filler dispersion and sufficient filler-matrix interaction, allowing effective stress transfer within the composite. However, untreated formulations show a steady, statistically validated decline at intermediate thresholds (group 'ab'), which worsens significantly as the loading increases. A major statistical drop is initiated at 15 wt.% treated (group 'b'), and the ultimate mechanical collapse is reached at 20 wt.% for both untreated and treated conditions, which are clustered together in the lowest homogeneous subset (group 'c'). This convergence suggests that increasing the filler loading beyond a certain threshold may adversely affect the composite structure, potentially due to reduced dispersion quality and increased filler-filler interactions. Under these conditions, the beneficial effect of alkali treatment appears to become less pronounced. This behavior is consistent with findings reported by (Karaoui et al., 2023) for untreated SCG in PP, and by (Safwan et al., 2013) for palm fruitlet fiber composites.

The strain values (Figure 6) decrease significantly upon SCG addition relative to neat PP (0.3366), confirming a significant brittle transition ($p < 0.001$; $F = 12.01$). Tukey's HSD test isolates the neat matrix at the apex of ductility (group 'a'), while a broad statistical overlap characterizes the majority of the loaded formulations. The 5 wt.% untreated formulation exhibits a significant initial drop, shifting to group 'b'. Interestingly, a wide, statistically homogeneous plateau (group 'bc') encompasses almost all other composites, spanning from low to high loadings regardless of treatment. A unique exception is observed at 15 wt.% untreated, which reaches a minimum elongation subset (group 'c'), suggesting a more restricted deformation capability, which may be associated with increased filler-filler interactions and reduced matrix mobility. The slight statistical variation and partial recovery noted at 20 wt.% treated (returning to group 'bc') may be related to local variations in the

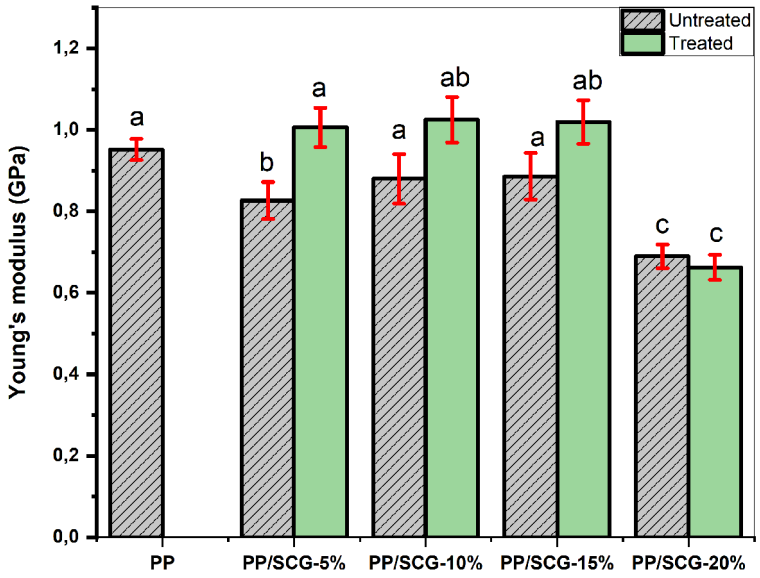

Figure 4. Young's modulus of PP/SCG biocomposites. Error bars represent standard deviations. Different letters indicate statistically significant differences (Tukey HSD, α = 0.05)

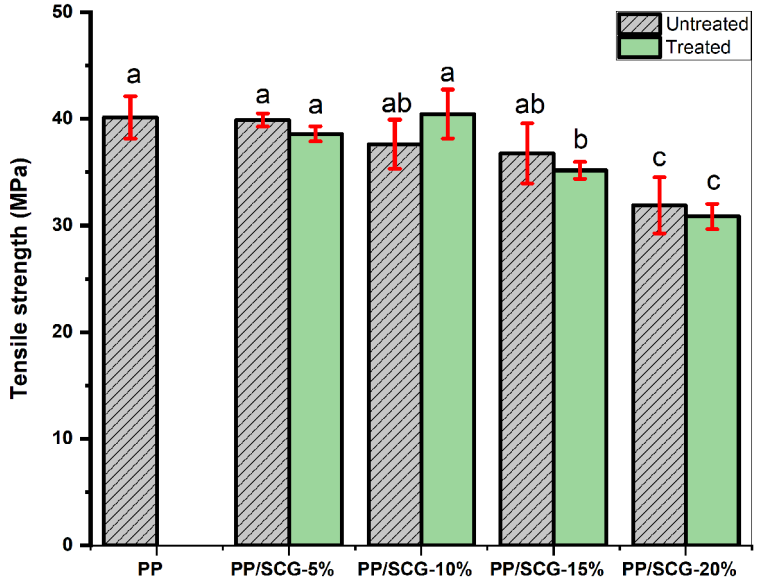

Figure 5. Tensile strength of PP/SCG biocomposites. Error bars represent standard deviations. Different letters indicate statistically significant differences (Tukey HSD, α = 0.05)

composite microstructure and stress distribution at high filler loading, a phenomenon similarly documented by (Karaoui et al., 2023) for PS/snail shell composites.

Hardness

Figure 7 shows a progressive increase in hardness as SCG content rises from 0% to 20%. The ANOVA framework validates that variations in SCG content induce a statistically significant modification of the material hardness ($p = 0.001$; $F = 5.57$). Pairwise comparisons reveal that lower filler contents (up to 10 wt.% treated and 5 wt.% untreated) remain statistically uniform and identical to the neat polymer matrix, sharing the baseline statistical family (group 'a'), suggesting that the filler contribution to surface rigidity is not yet dominant at these loadings. As the filler fraction increases, a structural transition zone emerges for 10 and 15 wt.% untreated (group 'ab'), before a sharp statistical enhancement is validated for the highly

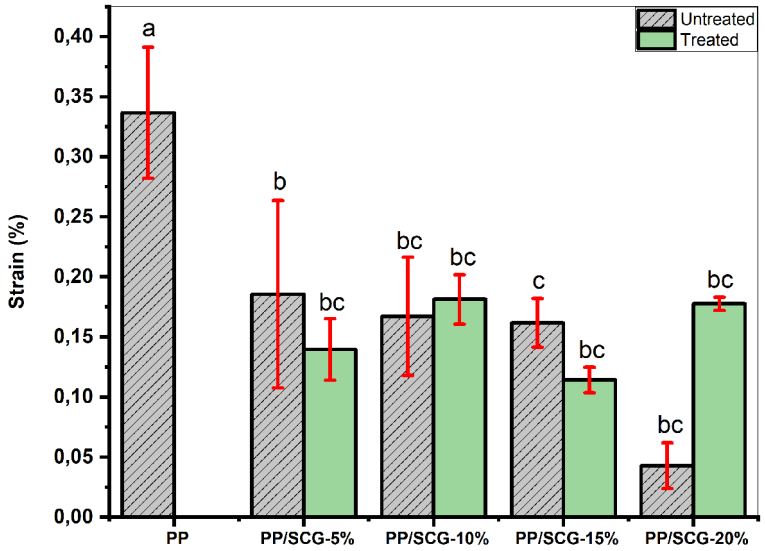

Figure 6. Strain of PP/SCG biocomposites. Error bars represent standard deviations. Different letters indicate statistically significant differences (Tukey HSD, α = 0.05)

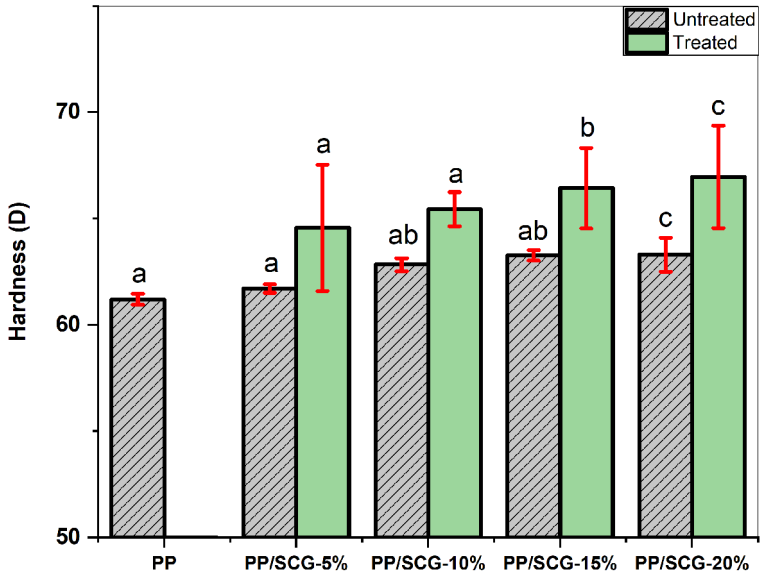

Figure 7. Shore D hardness of PP/SCG biocomposites. Error bars represent standard deviations. Different letters indicate statistically significant differences (Tukey HSD, α = 0.05)

loaded treated formulations. In fact, Tukey's test clusters the 15 and 20 wt.% treated composites within the highest hardness subsets (groups 'b' and 'c'). These observations are consistent with the findings of (Fernandes et al., 2022), who reported that alkali treatment significantly enhances hardness in PP composites reinforced with natural fibers. Similar trends were also reported by (Chakir, Alami, et al., 2024; Chakir, Mohamed, et al., 2024) for PP composites reinforced with calcium carbonate and wood flour filler, respectively.

Melt flow index

The rheological processability of the formulations was evaluated via MFI testing (Figure 8). One-way ANOVA confirmed that the compounding parameters severely alter the melt fluidity ($p < 0.001$; $F = 18.05$). Post-hoc Tukey's comparisons show that the neat PP possesses the absolute highest fluidity (group 'a'). Upon filler addition, the untreated composites show a gradual decrease in melt flow, transitioning to an intermediate plateau shared by most raw formulations (group 'b'). Pure PP exhibits the

highest flow rate (17.03 g/10 min). Upon the addition of untreated SCG, melt flow decreases to 11.76 g/10 min at 20 wt.% untreated. Crucially, alkali-treated composites display a significantly more severe drop in fluidity across all corresponding loading levels, collapsing to a minimum of 4.24 g/10 min at 20 wt.% treated (group 'c'). This pronounced rheological difference between untreated and treated composites suggests that alkali treatment substantially modifies the interactions between the filler and the polymer matrix. The stronger reduction in melt flow observed for treated SCG may be associated with enhanced filler–matrix interactions and increased resistance to polymer chain mobility within the molten composite. Statistically validated by the isolation of group 'c', this behavior demonstrates that the chemical removal of superficial hemicellulose and impurities successfully exposed the polar cellulose fibers. The observed decrease in flow may therefore result from a combination of increased filler-matrix interactions and the higher restriction imposed on polymer chain movement within the melt. Comparable patterns were reported in PP composites reinforced with agricultural waste fillers (Fayzullin et al., 2024; Zhiltsova et al., 2024), and the beneficial effect of alkali treatment on processability was confirmed by (Mohd Salehudiin et al., 2023) for kenaf-reinforced PP composites.

Density

Figure 9 shows that composite density rises progressively with SCG content ($p < 0.001$; $F = 23.18$). Tukey's multi-comparison test successfully organizes the density profiles into clear behavioral clusters. The neat PP matrix (0.904 g/ cm³), 5 wt% treated, and 5 wt% untreated formulations are grouped together in the lowest density family (group 'a'). This initial stability indicates that at low volumes, the filler is smoothly integrated without inducing immediate structural expansion. As expected, increasing the filler loading pushes the composites into statistically higher density subsets, peaking at 0.9610 g/ cm³ at 20 wt% untreated (group 'c'). This shift is mathematically driven by the high intrinsic density of the SCG bio-filler (~2.23 g/ cm³) compared to the raw PP matrix (~0.90 g/ cm³), adhering to the rules of spatial Rule of Mixtures (Gillespie et al., 2024). Interestingly, the alkali-treated composites display a systematically tighter and slightly lower density scale compared to their untreated counterparts. This high statistical reproducibility and the absence of erratic density spikes provide solid physical proof of a highly uniform filler dispersion; the chemical modification prevents random particle clustering, which in turn optimizes packing geometry and minimizes the inclusion of uncontrolled micro-voids at the interfacial boundaries (Fernandes et al., 2022).

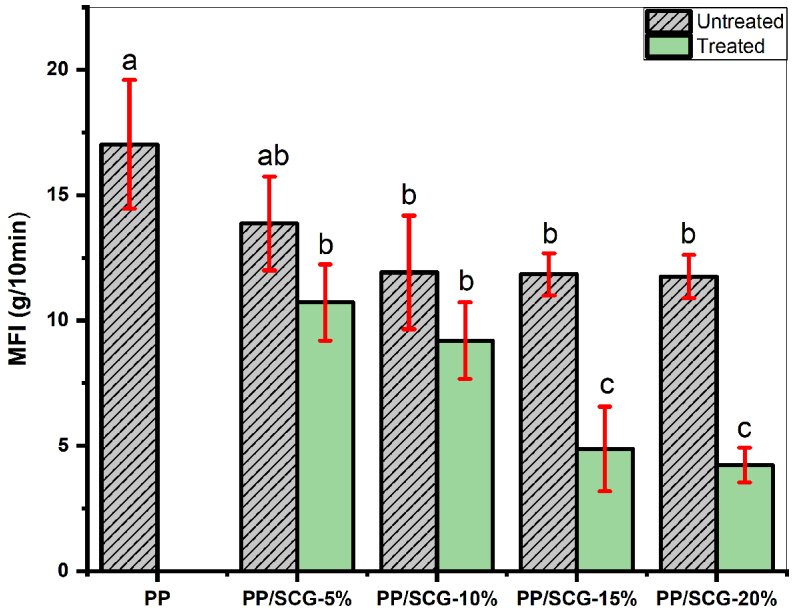

Figure 8. Melt flow index of PP/SCG biocomposites. Error bars represent standard deviations. Different letters indicate statistically significant differences (Tukey HSD, $\alpha = 0.05$)

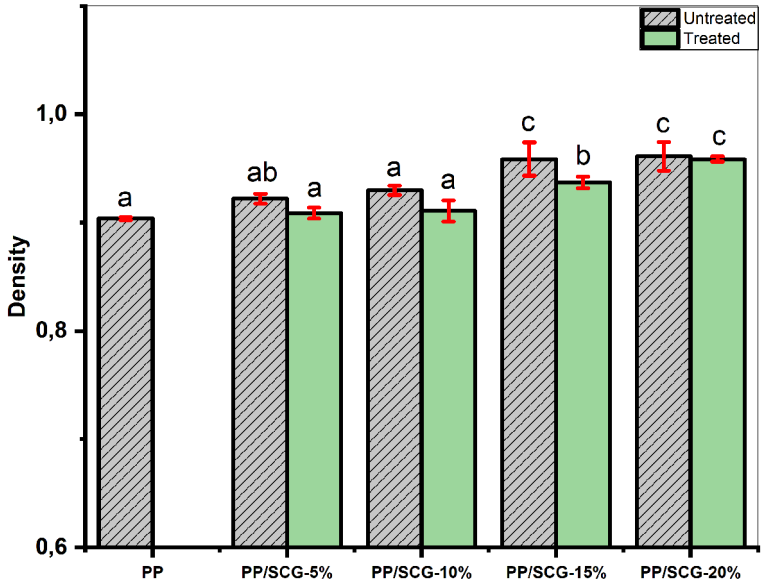

Figure 9. Density of PP/SCG biocomposites. Error bars represent standard deviations. Different letters indicate statistically significant differences (Tukey HSD, $\alpha = 0.05$)

Regression modeling analysis

Figures 10–13 present the regression analyses for all measured properties as a function of SCG content. Table 3 summarizes the R^2 values and best-fitting models for each property. Quadratic regression provides the highest R^2 values for most parameters, confirming the predominantly non-linear dependence of composite properties on filler content. This non-linearity reflects the complex interplay between filler content, matrix continuity, and interfacial interactions. In contrast, strain is best described by a linear model, suggesting a more uniform deformation response. Treated SCG composites generally exhibit higher R^2 values than untreated ones, indicating more predictable property evolution. The radar chart (Figure 14) further illustrates that treatment improves predictability for stiffness and density, while untreated composites better capture deformation-related behavior.

These observations are consistent with previous studies on PP-based natural fiber composites, where regression modeling has been used to predict mechanical performance and analyze the influence of filler content and treatment (Fernandes et al., 2022; Savran et al., 2022; Xiao et al., 2022).

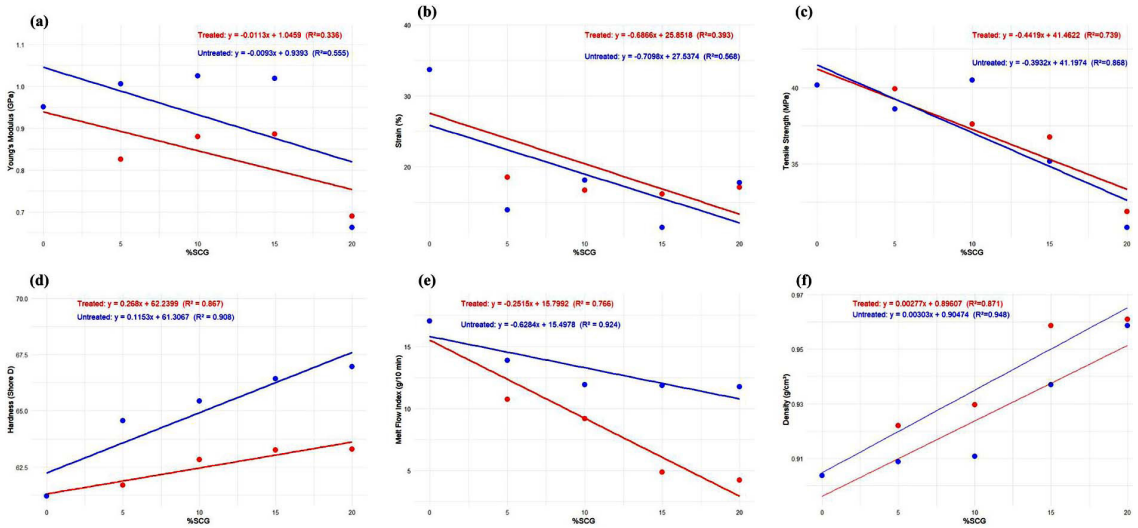

Figure 10. Linear regression of Young's modulus (a), strain (b), tensile strength (c), hardness (d), melt flow index (e), and density (f) of PP/SCG composites as a function of treated and untreated SCG content

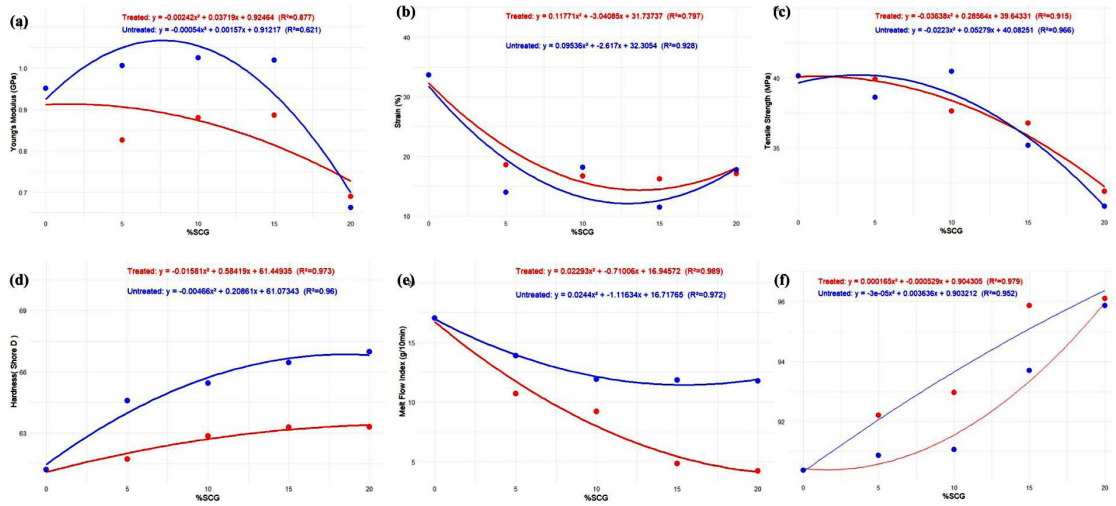

Figure 11. Quadratic regression of Young's modulus (a), strain (b), tensile strength (c), hardness (d), melt flow index (e), and density (f) of PP/SCG composites as a function of treated and untreated SCG content

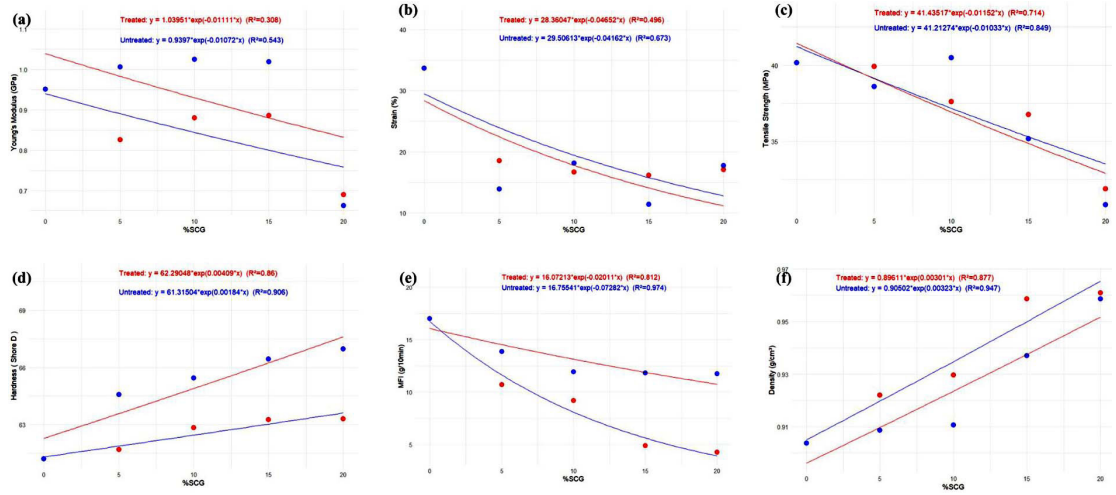

Figure 12. Exponential regression of Young's modulus (a), strain (b), tensile strength (c), hardness (d), melt flow index (e), and density (f) of PP/SCG composites as a function of treated and untreated SCG content

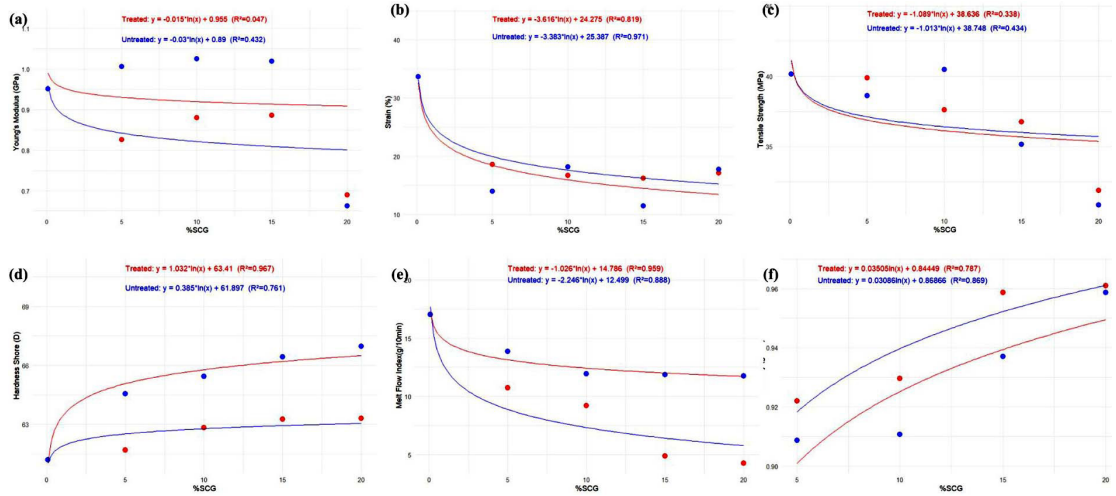

Figure 13. Logarithmic regression of Young's modulus (a), strain (b), tensile strength (c), hardness (d), melt flow index (e), and density (f) of PP/SCG composites as a function of treated and untreated SCG content

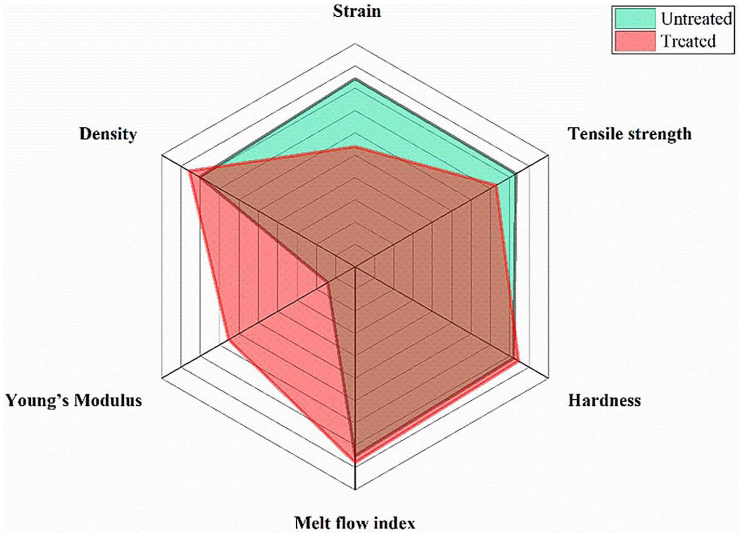

Figure 14. Radar plot of R^2 for PP/SCG composite properties

Table 3. Regression analysis results: coefficients of determination (R^2) for PP/SCG composites

Parameter	R^2		Equation (untreated)	Equation (treated)	Model
	Untreated	Treated			
Young's modulus	0.621	0.877	$y = -0.00054x^2 + 0.00157x + 0.00157$	$y = -0.00242x^2 + 0.03719x + 0.92464$	Quadratic
Strain	0.971	0.819	$y = -0.7098x + 27.5374$	$y = -0.6866x + 25.8518$	Linear
Tensile strength	0.966	0.915	$y = -0.0223x^2 + 0.05279x + 40.083$	$y = -0.0364x^2 + 0.2856x + 39.643$	Quadratic
Hardness	0.960	0.973	$y = -0.00466x^2 + 0.2861x + 61.073$	$y = -0.01581x^2 + 0.5841x + 61.449$	Quadratic
Melt flow index	0.974	0.989	$y = 0.0244x^2 - 1.1163x + 16.718$	$y = 0.0229x^2 - 0.7101x + 16.946$	Quadratic
Density	0.952	0.979	$y = -0.00003x^2 + 0.003636x + 0.903$	$y = 0.000165x^2 - 0.000529x + 0.904$	Quadratic

CONCLUSIONS

The experimental results confirm that SCG whether untreated or alkali-treated can be incorporated into PP at loadings up to 20 wt% without fundamentally compromising processability. One-way ANOVA confirmed statistically significant differences among all formulations for every measured property ($p < 0.05$), and post hoc Tukey HSD tests ($\alpha = 0.05$) revealed that alkali-treated composites at 5–15 wt% were statistically equivalent to neat PP in terms of stiffness, while the 20 wt% loading constituted a distinct threshold of property degradation for both treated and untreated systems.

Alkali treatment improved surface roughness and filler-matrix compatibility, translating into more stable mechanical behavior and better flow characteristics. With increasing filler content, hardness and density rose progressively while elongation at break declined, consistent with restricted mobility of polymer chains around rigid filler particles. Tensile strength remained close to neat PP at lower loadings (5–10 wt%) for treated composites. The reduction in MFI was more pronounced in treated composites (~75% at 20 wt%) than in untreated ones (~31%), confirming that stronger interfacial bonding restricts melt flow more significantly.

Quadratic regression models provided the best fit for most measured properties, reflecting the non-linear nature of filler-matrix interactions. Elongation at break followed a linear trend. Higher R^2 values for treated composites confirm that alkali treatment leads to more predictable and consistent property evolution. These findings confirm that SCG especially after alkali treatment represent a viable and sustainable biofiller for PP-based composites, and that regression modeling provides an effective quantitative framework for characterizing filler-content-dependent behavior within the 5–20 wt% loading range.

Acknowledgments

The authors acknowledge ENSAM, affiliated with University Moulay Ismail (UMI), for providing the academic and technical environment for this work. The first author gratefully acknowledges the financial support provided by the National Center for Scientific and Technical Research (CNRST) through the "PhD-Associate Scholarship – PASS" program in Morocco.

REFERENCES

1. Campos-Vega, R., Loarca-Piña, G., Vergara-Castañeda, H. A., Oomah, B. D. (2015). Spent coffee grounds: A review on current research and future prospects. *Trends in Food Science & Technology*, *45*(1), 24–36. https://doi.org/10.1016/j.tifs.2015.04.012
2. Chakir, A., Alami, M., Assouag, M., Noureddine, O., Elamarty, F. (2024). Effect of calcium carbonate as filler on the physicomechanical properties of polypropylene random. *International Journal of Engineering Research in Africa*, *69*, 1–17. https://doi.org/10.4028/p-s4CtdF
3. Chakir, A., Mohamed, A., Mohamed, A., El Amarty, F., Othmane, N. (2024). Utilization of wood flour waste as a filler on polypropylene random pipes industry. *Ecological Engineering & Environmental Technology*, *25*(7), 355–368. https://doi.org/10.12912/27197050/188736
4. Fayzullin, I., Gorbachev, A., Volfson, S., Serikbayev, Y., Nakyp, A., Akylbekov, N. (2024). Composite material based on polypropylene and modified natural fillers. *Polymers*, *16*(12), 1703. https://doi.org/10.3390/polym16121703
5. Fernandes, R., Da Silveira, P., Bastos, B., Da Costa Pereira, P., De Melo, V., Monteiro, S., Tapanes, N., Bastos, D. (2022). Bio-based composites for light automotive parts: statistical analysis of mechanical properties; effect of matrix and alkali treatment in sisal fibers. *Polymers*, *14*(17), 3566. https://doi.org/10.3390/polym14173566
6. Gillespie, A. K., Piskulich, Z. A., Knight, E., Prosniewski, M., Pfeifer, P. (2024). *Skeletal Density Measurements for Adsorbent Nanomaterials* (arXiv:2406.02762). arXiv. https://doi.org/10.48550/arXiv.2406.02762
7. Hernández-Varela, J. D., Medina, D. I. (2023). Revalorization of coffee residues: Advances in the development of eco-friendly biobased potential food packaging. *Polymers*, *15*(13), 2823. https://doi.org/10.3390/polym15132823
8. International Organization for Standardization. (2012). *ISO 527-2; Plastics—Determination of Tensile Properties—Part 2 Test Conditions for Moulding*.
9. International Organization for Standardization (ISO). (2003). *ISO868; Plastics and ebonite—Determination of indentation hardness by means of a durometer (Shore hardness). AFNOR: Paris, France, 2003.* https://www.iso.org/standard/34804.html
10. International Organization for Standardization (ISO). (2006). *EN ISO. 1183-1: 2006 Plastics—Methods for Determining the Density of Non-Cellular Plastics—Part 1: Immersion Method, Liquid Pyknometer Method and Titration Method.*
11. International Organization for Standardization (ISO). (2011). *ISO1133-2;Plastics—Determinationofthemeltmass-flowrate(MFR)andMeltVolume-FlowRate(MVR)ofThermoplastics—Part 2: Method for Materials with High Melt Flow Rates. ISO: Genva, Switzerland, 2011.*
12. International Organization for Standardization (ISO). (2022). *ISO 1133-1:2022 – Plastics—Determination of the melt mass-flow rate (MFR) and melt volume-flow rate (MVR) of thermoplastics—Part 1: Standard method*. https://www.iso.org/standard/83905.htm
13. Kamarudin, S. H., Mohd Basri, M. S., Rayung, M., Abu, F., Ahmad, S., Norizan, M. N., Osman, S., Sarifuddin, N., Desa, M. S. Z. M., Abdullah, U. H., Mohamed Amin Tawakkal, I. S., Abdullah, L. C. (2022). A review on natural fiber reinforced polymer composites (NFRPC) for sustainable industrial applications. *Polymers*, *14*(17), 3698. https://doi.org/10.3390/polym14173698
14. Kamarudin, S. H., Rayung, M., Abu, F., Ahmad, S., Fadil, F., Karim, A. A., Norizan, M. N., Sarifuddin, N., Mat Desa, M. S. Z., Mohd Basri, M. S., Samsudin, H., Abdullah, L. C. (2022). A review on antimicrobial packaging from biodegradable polymer composites. *Polymers*, *14*(1), 174. https://doi.org/10.3390/polym14010174
15. Karaoui, M., Fiore, V., Elhamri, Z., Kharchouf, S., Alami, M., Assouag, M. (2025). Study of the physico-chemical properties of injection-molded polypropylene reinforced with spent coffee grounds. *Journal of Composites Science*, *9*(6), 257. https://doi.org/10.3390/jcs9060257
16. Karaoui, M., Hsissou, R., Alami, M., Assouag, M. (2023). Thermal, flow, and mechanical properties of composites based on polystyrene (PS) and snail shell powder (SSP) biofiller (PS/SSP). *Iranian Polymer Journal*, *32*(5), 621–631. https://doi.org/10.1007/s13726-023-01151-2
17. Khoathane, M. C., Vorster, O. C., Sadiku, E. R. (2008). Hemp fiber-reinforced 1-pentene/polypropylene copolymer: the effect of fiber loading on the mechanical and thermal characteristics of the composites. *Journal of Reinforced Plastics and Composites*, *27*(14), 1533–1544. https://doi.org/10.1177/0731684407086325

18. Liao, Y., Wu, X., Peng, X., Zhou, Z., Wu, J., Wu, F., Jiang, T., Chen, J., Zhu, L., Yi, T. (2019). Enhancing the mechanical and thermal properties of polypropylene composite by encapsulating styrene acrylonitrile with ammonium polyphosphate. *BMC Chemistry*, *13*(1), 9. https://doi.org/10.1186/s13065-019-0534-6
19. McKay, I., Vargas, J., Yang, L., Felfel, R. M. (2024). A review of natural fibres and biopolymer composites: Progress, limitations, and enhancement strategies. *Materials*, *17*(19), 4878. https://doi.org/10.3390/ma17194878
20. Mohd Salehudiin, N., Salim, N., Roslan, R., Huda Abu Bakar, N., Noorbaini Sarmin, S. (2023). Improving the properties of kenaf reinforced polypropylene composite by alkaline treatment. *Materials Today: Proceedings*, *75*, 156–162. https://doi.org/10.1016/j.matpr.2022.11.089
21. Nurazzi, N. M., Asyraf, M. R. M., Fatimah Athiyah, S., Shazleen, S. S., Rafiqah, S. A., Harussani, M. M., Kamarudin, S. H., Razman, M. R., Rahmah, M., Zainudin, E. S., Ilyas, R. A., Aisyah, H. A., Norrrahim, M. N. F., Abdullah, N., Sapuan, S. M., Khalina, A. (2021). A review on mechanical performance of hybrid natural fiber polymer composites for structural applications. *Polymers*, *13*(13), 2170. https://doi.org/10.3390/polym13132170
22. Ortiz-Barajas, D. L., Arévalo-Prada, J. A., Fenollar, O., Rueda-Ordóñez, Y. J., Torres-Giner, S. (2020). Torrefaction of coffee husk flour for the development of injection-molded green composite pieces of polylactide with high sustainability. *Applied Sciences*, *10*(18), 6468. https://doi.org/10.3390/app10186468
23. Osman, Z., Elamin, M., Ghorbel, E., Charrier, B. (2025). Influence of alkaline treatment and fiber morphology on the mechanical, physical, and thermal properties of polypropylene and polylactic acid biocomposites reinforced with Kenaf, Bagasse, hemp fibers and softwood. *Polymers*, *17*(7), 844. https://doi.org/10.3390/polym17070844
24. Qaiss, A., Bouhfid, R., Essabir, H. (2015). Effect of Processing Conditions on the Mechanical and Morphological Properties of Composites Reinforced by Natural Fibres. In M. S. Salit, M. Jawaid, N. B. Yusoff, M. E. Hoque (Eds), *Manufacturing of Natural Fibre Reinforced Polymer Composites* (pp. 177–197). Springer International Publishing. https://doi.org/10.1007/978-3-319-07944-8_9
25. Raj, S. S. R., Dhas, J. E. R., Jesuthanam, C. (2021). Challenges on machining characteristics of natural fiber-reinforced composites – A review. *Journal of Reinforced Plastics and Composites*, *40*(1–2), 41–69. https://doi.org/10.1177/0731684420940773
26. Safwan, M. M., Sakhti, S. K., Ong, H. L., Hazizan, M. A., Anis Sofiah, M. K., Toh, G. Y. (2013). Preparation and characterization of polypropylene biocomposites reinforced palm fruitlet fiber. *Advanced Materials Research*, *795*, 281–285. https://doi.org/10.4028/www.scientific.net/AMR.795.281
27. Savran, M., Yılmaz, M., Öncül, M., Sever, K. (2022). Manufacturing and modeling of polypropylene-based hybrid composites by using multiple-nonlinear regression analysis. *Scientific Research Communications*, *2*(1), 1–15. https://doi.org/10.52460/src.2022.002
28. Serra-Parareda, F., Vilaseca, F., Aguado, R., Espinach, F. X., Tarrés, Q., Delgado-Aguilar, M. (2021). Effective young's modulus estimation of natural fibers through micromechanical models: the case of henequen fibers reinforced-PP composites. *Polymers*, *13*(22), 3947. https://doi.org/10.3390/polym13223947
29. Stelea, L., Filip, I., Lisa, G., Ichim, M., Drobotă, M., Sava, C., Mureșan, A. (2022). Characterisation of hemp fibres reinforced composites using thermoplastic polymers as matrices. *Polymers*, *14*(3), 481. https://doi.org/10.3390/polym14030481
30. Thanh, N. N., Tan, V. M., Trung, D. H., Huong, P. T. M., Nhung, L. T. H., Ha, N. M., Van, N. T., Tung, N. T.,Thuy, N. T. T. (2023). Effect of alkaline-treated spent coffee grounds and compatibilizer on the mechanical properties of bio-composite based on polypropylene matrix. *Vietnam Journal of Chemistry*, *61*(S3), 148–153. https://doi.org/10.1002/vjch.202300064
31. Väisänen, T., Haapala, A., Lappalainen, R., Tomppo, L. (2016). Utilization of agricultural and forest industry waste and residues in natural fiber-polymer composites: A review. *Waste Management*, *54*, 62–73. https://doi.org/10.1016/j.wasman.2016.04.037
32. Vigneshwaran, S., Sundarakannan, R., John, K. M., Joel Johnson, R. D., Prasath, K. A., Ajith, S., Arumugaprabu, V., Uthayakumar, M. (2020). Recent advancement in the natural fiber polymer composites: A comprehensive review. *Journal of Cleaner Production*, *277*, 124109. https://doi.org/10.1016/j.jclepro.2020.124109
33. Vilaseca, F., Valadez-Gonzalez, A., Herrera-Franco, P. J., Pèlach, M. À., López, J. P., Mutjé, P. (2010). Biocomposites from abaca strands and polypropylene. Part I: Evaluation of the tensile properties. *Bioresource Technology*, *101*(1), 387–395. https://doi.org/10.1016/j.biortech.2009.07.066
34. Xiao, X., Cheng, M., Zhong, Y. (2022). Effects of alkali treatment on the mechanical properties and moisture absorption behavior of flax/polypropylene composites. *Journal of Natural Fibers*, *19*(14), 9201–9222. https://doi.org/10.1080/15440478.2021.1982813
35. Zhiltsova, T., Campos, J., Costa, A., Oliveira, M. S. A. (2024). Sustainable polypropylene-based composites with agro-waste fillers: thermal, morphological, mechanical properties and dimensional stability. *Materials*, *17*(3), 696. https://doi.org/10.3390/ma17030696